# Revised perturbation theory for shifting geometric interfaces in high-contrast nanophotonics

Nathaniel Fried<sup>†</sup> and Avik Dutt\*,<sup>†</sup>,<sup>‡</sup>,<sup>¶</sup>

†Institute for Physical Science and Technology, University of Maryland, College Park,

Maryland 20742, United States

‡Department of Mechanical Engineering, University of Maryland, College Park, Maryland
20742, United States

¶National Quantum Lab at Maryland (QLab), College Park, Maryland 20740, United States

\* E-mail: avikdutt@umd.edu

### Abstract

Perturbation theory is a powerful technique for solving partial differential equations, efficiently bridging the gap between analytic solutions and numerical methods. While standard perturbation theory (SPT) is commonly applied in electromagnetism to account for the effects of small changes to material properties like nonlinear susceptibilities, losses, and thermo-optic effects, i.e. so called "bulk" perturbations, it is well-known to produce poor results when trying to account for small changes to the location of the boundaries between materials. This arises from the vectorial nature of boundary conditions in Maxwell's equations that are enforced at the location of the original boundary, and can not be "moved" via the process of linearly combining the original modes. We present an alternative formulation called pacified perturbation theory (PPT) which is able to account for this, and thus make accurate prediction of

both the effective indices and the mode profiles. We demonstrate this by benchmarking our proposed PPT using the case of a high-confinement multimode nanophotonic waveguide, and verify that the error associated with a first-order PPT approximation scales quadratically, unlike SPT (and its recent improvements) which fails to predict the changes in mode profiles to first order. We anticipate that our pacification procedure can be extended to higher-order corrections in perturbation theory, as well as broadened to fields beyond electromagnetism for computationally efficient predictions, where interfaces between dissimilar materials or the non-completeness of the original mode basis (e.g. for non-Hermitian systems) thwarts standard perturbation theory.

### **Keywords**

perturbation theory, nanophotonics, silicon photonics, multimode waveguides, coupled-mode theory

### Introduction

Perturbation theory is one of the key methods by which partial differential equations can be solved, bridging the gap between situations where analytic solutions can be found, and those where brute-force numerical techniques are required. It is often applied in quantum mechanics to find wavefunction solutions of the Schrödinger equation, but can be applied in electrodynamics<sup>1</sup> as well. While wavefunctions are usually either scalar or spinor fields, the electromagnetic field is a vector field, which poses unique challenges in systems lacking abundant geometrical symmetries.<sup>2</sup> In low-contrast/low-confinement or symmetric systems, the field can be approximated by a scalar, and the standard perturbation theory applies well. An example is the scalar basis of linearly polarized modes of an optical fiber.<sup>3-5</sup> However, in high-confinement systems like silicon photonics, <sup>6,7</sup> highly birefringent behavior results from the polarization dependence of the fields and the concomitant boundary

conditions for Maxwell's equations. These boundary conditions enforce the displacement field component perpendicular to the interface between two dielectrics to be continuous, which leads to the normal component of the electric field **E** in general being discontinuous (Fig. 1). Perturbation theory for electromagnetic fields has shown great success in modeling so-called "bulk" perturbations, <sup>8-11</sup> where the perturbation is present over a distributed region of space. Here the electromagnetic analogue of the usual perturbation theory from quantum mechanics correctly predicts the coupling between modes from the overlap integral of index perturbations introduced through nonlinear, thermo-optic, electro-optic or other means. <sup>12-16</sup> Standard perturbation theory (SPT) also works well for predicting coupling between well-separated waveguides, but fails in the case of narrowly separated high-confinement waveguides such as silicon slot waveguides. <sup>17</sup>

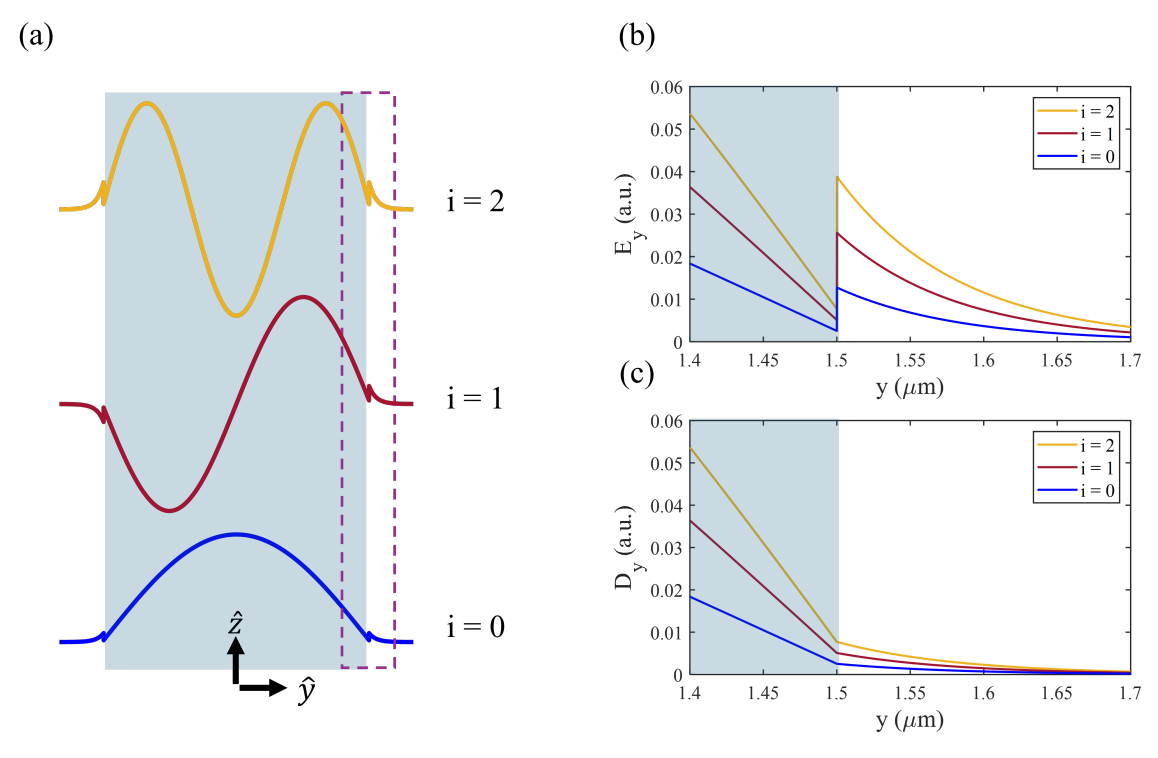


Figure 1: (a) Diagram of a slab waveguide and the amplitudes of the  $E_y$  component of the first 3 transverse magnetic (TM) modes. Depiction of the y components of the (b) E and (c) D fields (a.u.: arbitrary units) of the i=0, 1 and 2 modes of a representative silicon slab waveguide in the region near the core-cladding boundary indicated by the dashed rectangle in (a).

However, when one considers perturbations to the location of the interfaces between regions ("boundary perturbations"), <sup>2,8,9</sup> perturbation theory tends to produce poor results. It isn't well-defined since the coupling constants are computed via an integral of the electric and/or magnetic fields at the boundary. Even if the polarization is such that the relevant components are continuous, allowing one to do first-order perturbation theory, it will certainly not be differentiable, meaning second and higher order forms will fail. Examples of technologically relevant photonic structures that produce such shifting boundaries include optomechanical systems, <sup>18</sup> perturbed multimode waveguides, <sup>19–21</sup> alligator photonic crystal waveguides,  $^{22,23}$  and photonic crystal rings  $^{24-26}$  as opposed to the aforementioned nonlinear or electro-optic couplings which produce bulk perturbations. A more correct form of the coupling integral in these systems was determined by Johnson et al.<sup>27</sup> by considering the limit of a series of anisotropically smoothed systems, and is effective for computing changes in the eigenvalues of resonant systems (such as the mode effective indices  $n_{\rm eff}$ , propagation constants  $\beta$ , or resonant frequencies  $\omega$ ). 25,28–30 We will refer to this improved version of SPT as SPT+ in this work. However, as Johnson et al. comment in their paper, 27 "the standard perturbation theory method for computing first-order eigenfields and higher-order eigenvalue corrections rely on one key assumption that is false for Maxwell's equations: they assume that the basis of the unperturbed eigenstates is complete." This leads to substantial error in the prediction of the new fields between the locations of the original and updated boundaries. Thus, there is a need for a revised perturbation theory that makes corrections to the unperturbed mode profiles.

The problems caused by interface discontinuities also appear when determining the 3D modes of a resonant structure, and have been addressed in manners similar to what we will be presenting in this work. Rather than trying to claim that the original and updated mode profiles can be approximated by each other, one can use the assumption that only the components of the E field parallel to the interface  $E_{||}$  are approximately equal, and that instead the component of the D fields perpendicular to the interface  $D_{\perp}$  are approximately equal.

Another method approximates the part of the mode profiles between the perturbed and original boundaries via a Taylor series. <sup>31</sup> Both of these methods were able to make improvements by adjusting the mode profiles between the interfaces to account for the discontinuities of the electric field at the boundary. As a result of this, both were able to make reasonable predictions for the eigenvalues and coupling constants; however, neither went so far as to estimate the mode profiles and their error scaling behavior.

Our solution is to instead create an isomorphism  $P_{\vec{R}}: |\psi\rangle \to |\tilde{\psi}\rangle$  where  $|\tilde{\psi}\rangle$  is a quantity that does vary smoothly in respect to the perturbations of a set of parameters  $\vec{R}$  that define the properties of the system in question. We dub  $|\tilde{\psi}\rangle$  as the "pacified" mode profiles, and  $P_{\vec{R}}$  as the "pacification" operator. If we want to know the mode profiles and indices corresponding to a set of parameters  $\vec{R}'$ , and we know the mode profiles at another similar set of parameters  $\vec{R}_0$  (the "base" mode profiles), the path is simple: we can transform the mode to the pacified basis, apply the perturbation, and then transform it back to the original basis.

Our pacified perturbation theory (PPT) is able to accurately estimate both the mode profiles and indices over a range of perturbation strengths, unlike SPT+ which can only accurately estimate the mode indices, as we will demonstrate. We benchmark PPT using a scenario with exact analytical solutions – the slab waveguide, and explicitly show a second order scaling of the mean squared error (MSE) in the mode profiles via our improved PPT, as compared to a first-order scaling observed in SPT and SPT+. While we only show second-order scaling here, we believe a more sophisticated pacification operation could enable a higher-order PPT to be developed.

Note that an alternative method to formulate a coupled-mode theory (CMT) is to represent the perturbation not as a change in the permittivity, but instead as a change in a curvilinear coordinate system, <sup>32–34</sup> similar to the methods of transformation optics. <sup>35</sup> This results in the perturbation being "converted" from a boundary perturbation to a bulk perturbation. However, this method comes with a significant complexity cost, as the coupling

integrand will be non-zero at all points in the cross section and may also result in an effectively anisotropic and non-constant permittivity/permeability, significantly increasing the number of calculations needed to determine the coupling constants. Hence the improved PPT approach we introduce in this work has advantages over coordinate transformation methods, especially when extended to higher-order methods.

### Theory

Consider a photonic structure that hosts a set of transverse modes that are propagating in the +z direction whose transverse index profile may or may not be altered (for example, a multimode waveguide or optical fiber). To determine the modes of such a structure, we will start with following formulation of Maxwell's equations:  $^{32}$ 

$$-ig\partial_z |\psi\rangle = L |\psi\rangle \tag{1}$$

where the operators L, g, and mode profile vector  $|\psi\rangle$  are defined as

$$g = \begin{pmatrix} 0 & -\hat{z} \times \\ \hat{z} \times & 0 \end{pmatrix} \quad L = \begin{pmatrix} \epsilon - \nabla_t \times (\hat{z} \, (\hat{z} \cdot \nabla_t \times)) & 0 \\ 0 & 1 - \nabla_t \times \left(\frac{1}{\epsilon} \hat{z} (\hat{z} \cdot \nabla_t \times)\right) \end{pmatrix} \quad |\psi\rangle = \begin{pmatrix} \vec{E}_t \\ \vec{B}_t \end{pmatrix} \tag{2}$$

where  $\nabla_t$ ,  $\vec{E}_t$ , and  $\vec{B}_t$  are the projections of the gradient operator, and the electric and magnetic fields onto the transverse (x and y) plane. Note that we have made redefinitions to the  $\nabla_t$  and  $\partial_z$  operators and spatial coordinates to make various factors of the wavenumber k disappear, which is equivalent to measuring distances in units of  $\frac{1}{k}$ . Additionally,  $\epsilon$  is the relative permittivity profile of the waveguide's cross section, which could potentially be complex to account for losses and non-Hermitian behavior, and in principle could be anisotropic as well.

A generalized eigenstate i (the pairing of an eigenfunction  $|\psi_i\rangle$  and eigenvalue  $n_i$ , that

we will refer to as the mode profiles and mode indices respectively) satisfies the following condition by definition.<sup>36</sup>

$$n_i g |\psi_i\rangle = L |\psi_i\rangle \tag{3}$$

Since the g and L operators are both symmetric, the mode profiles are orthogonal over the cross section of the waveguide<sup>37–39</sup> and can be taken to be of unit norm:

$$\langle \psi_i | g | \psi_j \rangle = \int dx dy \ \hat{z} \cdot \left( E_t^i \times B_t^j + E_t^j \times B_t^i \right) = \delta_{ij}$$
 (4)

The g operator thus serves as a metric on the space of mode profiles. For modes with a component perpendicular to the surface being shifted, between the original and perturbed boundaries, there will always be a jump proportional to the change in index and the component of the D field perpendicular to the boundary, thus the change in the modes is not first order, but zeroth order. We must find a way to properly account for the zeroth order change in the modes to have a proper perturbation theory. Another way of saying this is that the perturbed modes are not within the span of the original modes; they do not form a valid basis except when the index profile is identical to what it was originally. It is possible that if one were to utilize a large amount of unbound modes to improve a basis, the convergence of the expansion might improve, however it would only be in a least-squares sense, since there would inevitably be the Gibbs phenomenon around the location of the discontinuities.

If the index profile is controlled by a set of parameters  $\vec{R}$  (i.e. the locations of the boundaries, or the width and center location), we can say that that is a problem of determining how to parallel transport<sup>40</sup> vectors (the mode profiles) in the space of parameters. To do this, we instead define a similar perturbation theory for the "pacified" mode profiles.

Rewriting Eq. (3) in terms of the pacified mode profiles and additionally applying the inverse pacification operator  $P^{-1}$  gives us:

$$n_i P^{-1}gP^{-1}|\tilde{\psi}_i\rangle = P^{-1}LP^{-1}|\tilde{\psi}_i\rangle \tag{5}$$

We can then define pacified operators  $\tilde{g}$  and  $\tilde{L}$  as

$$\tilde{g} = P^{-1}gP^{-1} \quad \tilde{L} = P^{-1}LP^{-1}$$
 (6)

Note that this makes  $\tilde{g}$  an operator that varies throughout parameter space, unlike its unpacified counterpart. As such, additional terms will appear in PPT corresponding to the changes in the metric that we refer to as rescaling terms. We can then take a gradient in respect to the parameters  $\vec{R}$  and apply an arbitrary bra to get the equation:

$$\nabla_{\vec{R}} n_j \, \delta_{ij} + n_j \, \langle \tilde{\psi}_i | \, \nabla_{\vec{R}} \tilde{g} \, | \tilde{\psi}_j \rangle - \langle \tilde{\psi}_i | \, \nabla_{\vec{R}} \tilde{L} \, | \tilde{\psi}_j \rangle = (n_i - n_j) \, \langle \tilde{\psi}_i | \, \tilde{g} \, | \nabla_{\vec{R}} \tilde{\psi}_j \rangle \tag{7}$$

We define the "total" perturbation matrix elements as  $\vec{M}_{ij} = \langle \tilde{\psi}_i | \nabla_{\vec{R}} \tilde{L} | \tilde{\psi}_j \rangle - n_j \langle \tilde{\psi}_i | \nabla_{\vec{R}} \tilde{g} | \tilde{\psi}_j \rangle$  since they play the same role as the perturbation matrix elements of SPT (just  $\langle \tilde{\psi}_i | \nabla_{\vec{R}} \tilde{L} | \tilde{\psi}_j \rangle$ ), but with the additional rescaling terms added in. We can identify the eigenvalue shifts by taking i = j, giving us

$$\nabla_{\vec{R}} n_i = \vec{M}_{ii} \tag{8}$$

If we assume  $i \neq j$ , then we can infer

$$\langle \tilde{\psi}_i | \, \tilde{g} \, | \nabla_{\vec{R}} \tilde{\psi}_j \rangle = -\frac{\vec{M}_{ij}}{n_i - n_j} \tag{9}$$

These last two equations are the PPT analogues of what is commonly referred to as the first and second Hellmann-Feynman theorems respectively.<sup>41</sup>

We can reconstruct  $|\nabla_{\vec{R}}\tilde{\psi}_j\rangle$  via a resolution of the identity over all relevant modes, remembering that the inner product is defined with the metric g:

$$|\nabla_{\vec{R}}\tilde{\psi}_{j}\rangle = \sum_{i} |\tilde{\psi}_{i}\rangle \langle \tilde{\psi}_{i}| \,\tilde{g} \,|\nabla_{\vec{R}}\tilde{\psi}_{j}\rangle = |\tilde{\psi}_{j}\rangle \langle \tilde{\psi}_{j}| \,\tilde{g} \,|\nabla_{\vec{R}}\tilde{\psi}_{j}\rangle - \sum_{i\neq j} |\tilde{\psi}_{i}\rangle \frac{\vec{M}_{ij}}{n_{i} - n_{j}}$$
(10)

Note that this is the step where SPT would fail, as it assumes that the mode at R' can be

represented in terms of the profiles at  $R_0$ . In order to determine the self-coupling, we must turn to our normalization condition Eq. (4). Applying the parameter gradient gives:

$$\langle \tilde{\psi_j} | \, \tilde{g} \, | \nabla_{\vec{R}} \tilde{\psi_j} \rangle + \langle \nabla_{\vec{R}} \tilde{\psi_j} | \, \tilde{g} \, | \tilde{\psi_j} \rangle + \langle \tilde{\psi_j} | \, \nabla_{\vec{R}} \tilde{g} \, | \tilde{\psi_j} \rangle = 0$$

Therefore

$$\operatorname{Re}\left(\langle \tilde{\psi}_{j} | \, \tilde{g} \, | \nabla_{\vec{R}} \tilde{\psi}_{j} \rangle\right) = -\frac{1}{2} \, \langle \tilde{\psi}_{j} | \, \nabla_{\vec{R}} \tilde{g} \, | \tilde{\psi}_{j} \rangle \tag{11}$$

We set the imaginary part of the self-coupling, corresponding to phase rotations throughout the parameter space (a free parameter), to be zero. This makes the overall mode profile evolution equation:

$$|\nabla_{\vec{R}}\tilde{\psi}_{j}\rangle = -\frac{1}{2} |\tilde{\psi}_{j}\rangle \langle \tilde{\psi}_{j}| \nabla_{\vec{R}}\tilde{g} |\tilde{\psi}_{j}\rangle - \sum_{i \neq j} |\tilde{\psi}_{i}\rangle \frac{\vec{M}_{ij}}{n_{i} - n_{j}} = -\sum_{i} |\tilde{\psi}_{i}\rangle \vec{x}_{ij}(\vec{R})$$
(12)

where  $\vec{x}_{ij}$  are the coupling coefficients of the modes in respect to  $\vec{R}$ , and are defined via the above equation. For a first-order approximation of the mode profiles at  $\vec{R}$  from the base mode profiles at  $\vec{R}_0$ , the new pacified mode profiles would be

$$|\tilde{\psi}_{j}(\vec{R}')\rangle \approx |\tilde{\psi}_{j}(\vec{R}_{0})\rangle - \sum_{i} |\tilde{\psi}_{i}\rangle \,\vec{x}_{ij}(\vec{R}_{0}) \cdot (\vec{R}' - \vec{R}_{0})$$
 (13)

We parameterize the state of a waveguide by two values: s, the location of the center of the waveguide, and w, half the width of the overall waveguide. Parameterizing this way, as opposed to the locations of the two boundaries, has the benefit of rendering the operations of changing the two parameters (depicted in Fig. 4(a) and 4(b)), which we will refer to as "shifts" and "dilations", to have odd and even parity respectively. This means that only cross-parity mode coupling can occur via a shift and only same-parity modes can be coupled via a dilation.

Once a valid pacification operation and a set of base mode indices/profiles are defined,

these equations form a system of nonlinear PDEs for the mode profiles that can theoretically be solved by standard numerical methods. For this work, we will examine transverse magnetic (TM) modes in a slab waveguide since the modes have closed-form expressions that allow us to easily compare the estimated mode profiles to the exact ones. Restricting to one polarization means that only the  $E_y$ ,  $B_x$  and  $E_z$  fields are ever non-zero, so we only have to account for 2 of the four components of  $|\psi\rangle$  ( $E_z$  is constrained to always be  $\frac{1}{i\epsilon}\partial_y B_x$  in this formulation). The pacification we will use is the following matrix which converts the  $E_y$  component (the direction perpendicular to the interface) to the  $D_y$  component.

$$P = \begin{pmatrix} 1 & 0 & 0 & 0 \\ 0 & \epsilon & 0 & 0 \\ 0 & 0 & 1 & 0 \\ 0 & 0 & 0 & 1 \end{pmatrix} \tag{14}$$

Thus the variables of relevance are  $D_y$  and  $B_x$ , both of which are continuous at the interface. The perturbation matrix elements  $\langle \tilde{\psi}_i | \nabla_{\vec{R}} \tilde{L} | \tilde{\psi}_j \rangle$  when evaluated straightforwardly are:

$$\langle \tilde{\psi}_i | \nabla_{\vec{R}} \tilde{L} | \tilde{\psi}_j \rangle = -\int dy \, \nabla_{\vec{R}} \epsilon \frac{D_y^i}{\epsilon} \frac{D_y^j}{\epsilon} + B_x^i \partial_y \left( \nabla_{\vec{R}} \left( \frac{1}{\epsilon} \right) \partial_y B_x^j \right)$$
 (15)

However, this integral is not well-defined when we consider  $\epsilon$  as a discontinuous function, since we must evaluate the values of the  $\epsilon$  and the derivatives of the magnetic field on the boundary despite those quantities being discontinuous there. This can be fixed by utilizing integration by parts on the second term (boundary term is zero), and using the backwards derivative chain rule on the first term, resulting in:

$$\langle \tilde{\psi}_i | \nabla_{\vec{R}} \tilde{L} | \tilde{\psi}_j \rangle = \int dy \, \nabla_{\vec{R}} \left( \frac{1}{\epsilon} \right) D_y^i D_y^j - \nabla_{\vec{R}} \epsilon \, \frac{\partial_y B_x^i}{\epsilon} \frac{\partial_y B_x^j}{\epsilon} \tag{16}$$

The last term can also be simply recognized as the product of the  $E_z$  components via the previously mentioned identity for  $E_z$ . Thus the values in the integrand are all continuous

functions except for the  $\nabla_{\vec{R}}\epsilon$  and  $\nabla_{\vec{R}}\left(\frac{1}{\epsilon}\right)$  terms which are proportional to Dirac delta functions, forcing the integral to be evaluated purely on the boundary. Similarly, the  $\langle \tilde{\psi}_i | \tilde{g} | \tilde{\psi}_j \rangle$  matrix elements can be shown to be:

$$\langle \tilde{\psi}_i | \nabla_{\vec{R}} \tilde{g} | \tilde{\psi}_j \rangle = -\int dy \, \nabla_{\vec{R}} \left( \frac{1}{\epsilon} \right) \left( D_y^i B_x^j + B_y^i D_x^j \right) \tag{17}$$

we can write simplified versions of the total perturbation matrix elements  $\vec{M}_{ij}$  by using the following identity.

$$B_x^i = -\frac{D_y^i}{n_i} \tag{18}$$

substituting Eq. (18) into (17), the total perturbation matrix elements  $\vec{M}_{ij}$  become

$$M_{ij} = -\int dy \, \frac{n_j}{n_i} \nabla_{\vec{R}} \left(\frac{1}{\epsilon}\right) D_y^i D_y^j + \nabla_{\vec{R}} \epsilon \, E_z^i E_z^j \tag{19}$$

As such, our method's approximation of the first-order index shifts is identical to that of  $^{27}$  since the extra factor of  $\frac{n_j}{n_i}$  will be equal to one for the diagonal terms. We choose to represent the mode profiles with  $D_y$  and  $E_z$  since that way, another derivative doesn't need to be taken in the computation of the perturbation matrix elements which would lead to more differentiability issues. In practice, this means that the estimated profiles will be formed by linearly combining the  $D_y$  and  $E_z$  functions of the different modes, rather than the  $D_y$  and  $B_x$  functions.

### Results

We will examine the modes of a prototypical Si-SiO<sub>2</sub> slab waveguide ( $\lambda = 1.55\mu$ m, width =  $3\mu$ m,  $n_{core} = 3.46$   $n_{clad} = 1.53$ ) in this section, comparing the estimations made with PPT with three others methods: SPT, SPT+, and the base mode profiles/indices. Taking the updated mode profiles/indices to be like the base mode profiles is effectively the 0th order approximation from all three of these methods, and provides a reference for how much the

total variations of the modes are.

This waveguide has 12 bound modes, which will be the only modes we will consider in this work. The perturbative adjustments to and from unbound modes could be determined by PPT as well, but it would introduce complications that are not important to demonstrate the efficacy of PPT. The unbound modes cannot be simply normalized as they are not confined to a compact region, and thus require a regularization scheme <sup>42</sup> like the implementation of perfectly matched layers (PMLs). The unbound modes are important in computing the adjustments to weakly-confined modes as well as for the accounting of leakage to radiation modes. <sup>38</sup> In turn, we will restrict our attention to the first few well-confined modes of this waveguide.

Fig. 2 depicts the coupling per unit change in w (top row) and s (bottom row) between the bound modes of this waveguide. The values of  $\vec{x}_{ij}$  for both SPT+ (Fig. 2(a,e)) and PPT (Fig. 2(b,f)) are depicted, as well as the differences between PPT and SPT+ (Fig. 2(c,g)) and the differences between SPT+ and SPT (Fig. 2(d,h)). Since the perpendicular electric field is not well defined on the boundary, to enable SPT to make some prediction, we opted to use the average of its value on each side of the boundaries as an ad-hoc approximation in the evaluation of SPT's coupling coefficients. While the differences tend to be proportional to the size of the coupling coefficients themselves (especially for SPT/SPT+), the rescaling term introduces two important differences between PPT and SPT. Firstly, the factor of  $n_j$  attached to the rescaling term breaks the symmetry between i and j, rendering  $x_{ij}$  non-symmetric, resulting in greater differences between PPT and SPT+ when  $i \ll j$ . Additionally, the rescaling terms cause there to be self-coupling present when the waveguide is dilated.

In each of the estimation schemes, there is a finite amount of error localized between the old and new locations of the boundary due to the discontinuous behaviour at the boundary, as depicted in Fig. 3. For SPT, SPT+, and the base modes, this region is roughly rectangular with a height of approximately  $\Delta(1/\epsilon)D_y(\frac{w}{2})$ , whereas for PPT, this region is a triangle whose *slope* is proportional to the difference in the derivatives of  $D_y$  on either side of the

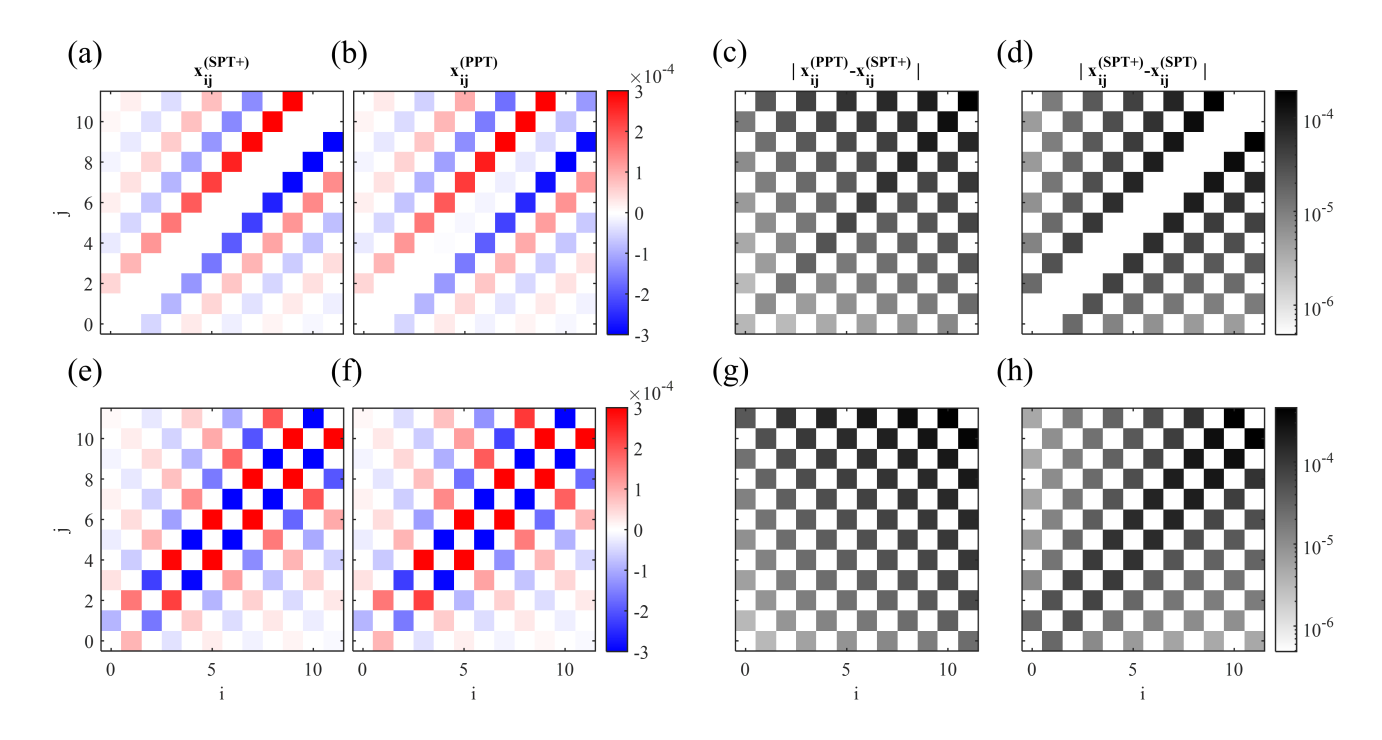


Figure 2: Coupling coefficient predictions (based on Eq. (12)) via SPT+ (a,e), PPT (b,f), the differences between SPT+ and PPT (c,g), and the differences between SPT+ and SPT. Coefficients are given in units of 1/nm in respect to both a dilation (a-d) and a shift (e-h). Note that the colorbar axes in (c,d,g,h) are in log scale.

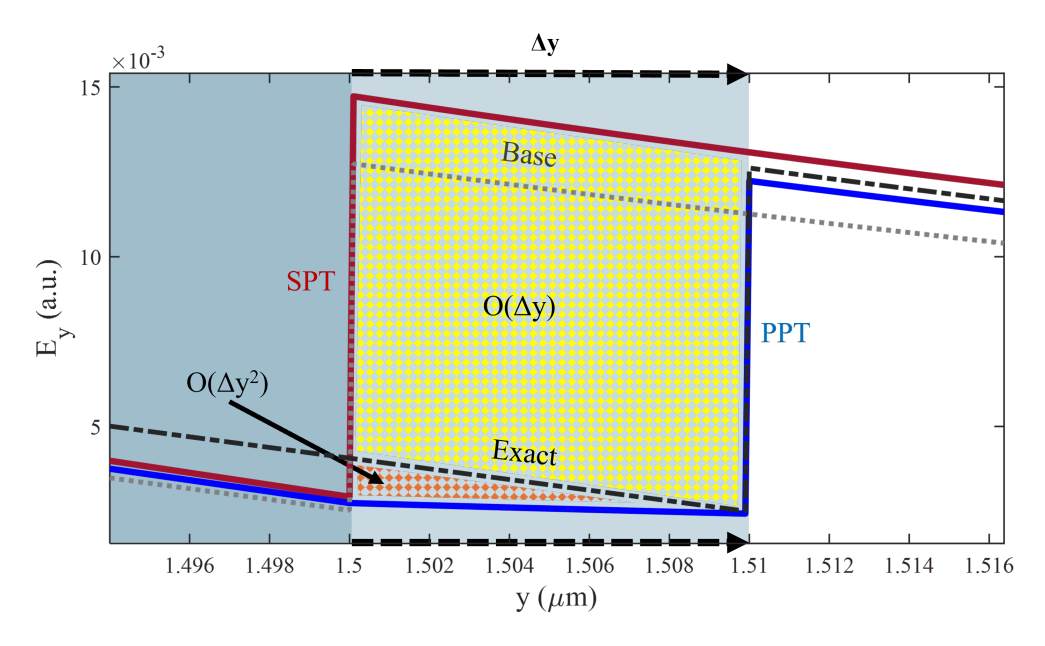


Figure 3: Diagram indicating the boundary-localized error error in the SPT and PPT approximations (a.u.: arbitrary units) after a waveguide is shifted by 10 nm to the right. The region between the exact mode profile and the SPT estimate forms a rectangle (yellow), whereas the region between the exact mode profile and the PPT estimate takes the form of a triangle (orange). The areas scale differently with the size of the perturbation  $\Delta y$ , and so does the amount of error. Additionally, it is clear that the SPT estimate is much closer to the base mode profile between the boundaries than it is to exact mode profile, but the opposite is true for the PPT estimate.

boundaries  $|\Delta \epsilon E_z(\frac{w}{2})|$ . Since both have a base width of  $\Delta y$ , the area of the error region in the SPT approaches will scale with  $\Delta y$  whereas the area in PPT will scale with  $\Delta y^2$ . We can think of the overall error as a combination of the boundary-localized error and the bulk error which is distributed over the space. Since the overall error scaling is determined by what the lowest-order contribution to the error is, SPT (and SPT+) should scale at most linearly, since the boundary-localized error scales linearly. PPT however should be able to scale quadratically since both the bulk and boundary contribute error that scales quadratically. While the bulk error can presumably be reduced by carrying out the normal steps of a second or higher-order perturbation theory, the boundary error will be left unaffected, as it is "built-in" to the modes themselves, rendering the reduction in bulk error irrelevant or impossible. This also means that a second order PPT (where error scales cubically) can not be created with this pacification operator, but we are actively exploring other possible

pacification operations that would enable higher-order perturbation theory.

For a perturbation theory to be useful, it must locally scale at least quadratically so that the error in approximating the modes a fixed distance away in parameter space scales linearly with the step size, and thus is minimizable to within a desired degree.

We compute the MSE of the mode profiles as follows, keeping in mind the metric g for the inner products between vectors in the standard (g = 1) and the pacified spaces:

$$\||\psi_i\rangle - |\psi_i^{(exact)}\rangle\|^2 = \left(\langle\psi_i| - \langle\psi_i^{(exact)}|\right)g(|\psi_i\rangle - |\psi_i^{(exact)}\rangle)$$
(20)

To determine the effective "order" of each form of perturbation theory, we calculate the MSE in each case of the mode profiles (all calculations from this work were performed in MATLAB) upon the application of a shift or dilations between 1Å and 80 nm. The error data is then fit to a power law  $a(\Delta y)^b$  where a and b are fit constants, with b being the effective order plus one. The fit is restricted to small perturbations (<5 nm) to identify the power of only the lowest-order contribution in the Taylor series, as the contributions of the higher order error terms only matter for large perturbations. As a first example, we calculate the error scaling of the mode profile for a shift in the multimode waveguide while maintaining the same width. Since shifts can not couple modes to themselves, they will not lead to changes in the eigenvalues. This is intuitively correct considering the translational symmetry of the original problem: when we shift a waveguide, we should expect the propagation constants to stay the same and the mode profiles to simply shift along with the waveguide. In Fig. 4(c), the MSE for each of the approximations of the fundamental mode of the slab waveguide over the various size regimes is depicted. It is evident that both SPT and SPT+ provide little gain over the base mode profiles for  $\Delta w < 10$  nm, and SPT+ provides little gain over SPT except for  $\Delta w > 10$  nm. Only for large perturbation where the higher-order contributions start to dominate is there any benefit in using SPT and SPT+ over the base mode profiles.

In contrast, PPT provides a reduction by 1-3 orders of magnitude for small shifts, and

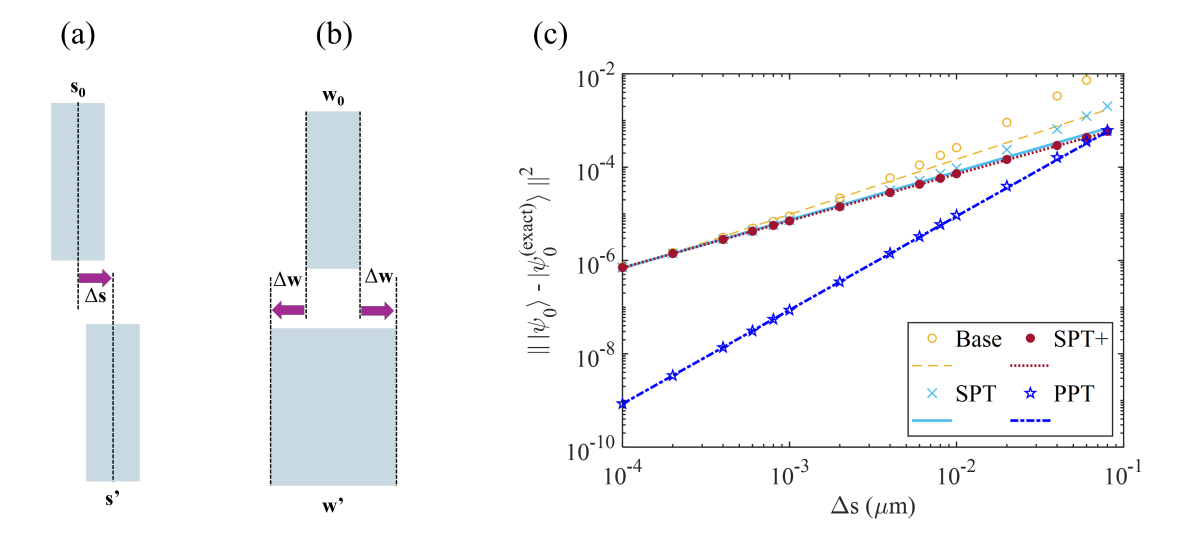


Figure 4: (a) Pictorial representation of a shift of the waveguide by  $\Delta s$ . (b) Pictorial representation of a dilation of the waveguide by  $\Delta w$ . (c) Mean square error (MSE) of the Base, SPT, SPT+, and PPT estimations of the fundamental transverse magnetic mode profiles (TM0) for shifts (as in (a)). The approximations scale by exponents of 1.182, 1.032, 1.003, and 2.010 respectively. SPT: standard perturbation theory. PPT: pacified perturbation theory. SPT+ stands for the recent improvements to SPT.

closely adheres to the quadratic scaling relation all the way to the 80-nm mark. We next compare the estimation schemes for dilations of the waveguide width, which produce changes in both the eigenvalues  $n_i$  and the eigenmodes  $|\psi_i\rangle$  in Fig. 5. Compared to center shifts, dilations provide an additional check in the form of the mode index shifts, whereby the error is defined as the absolute value of the difference between predicted and exact values. Since the eigenvalue prediction for PPT is exactly identical to that of SPT+, we will only draw one curve for PPT. While the averaging-based SPT provides a slight improvement to the mode index, the error still scales linearly, whereas PPT scales quadratically as expected. The MSE graphs in Fig. 5 tell a similar story as to Fig. 4, except that SPT and the base mode profiles seem to have less error, further shrinking the error reductions by SPT and SPT+.

Finally, if we apply a perturbation theory to a higher-order mode, we expect that there will be more error since there are only a finite number of bound states to represent their changes; higher modes will have less modes available to couple to and thus more error. Despite this caveat, we show that PPT also works well to represent the changes of the

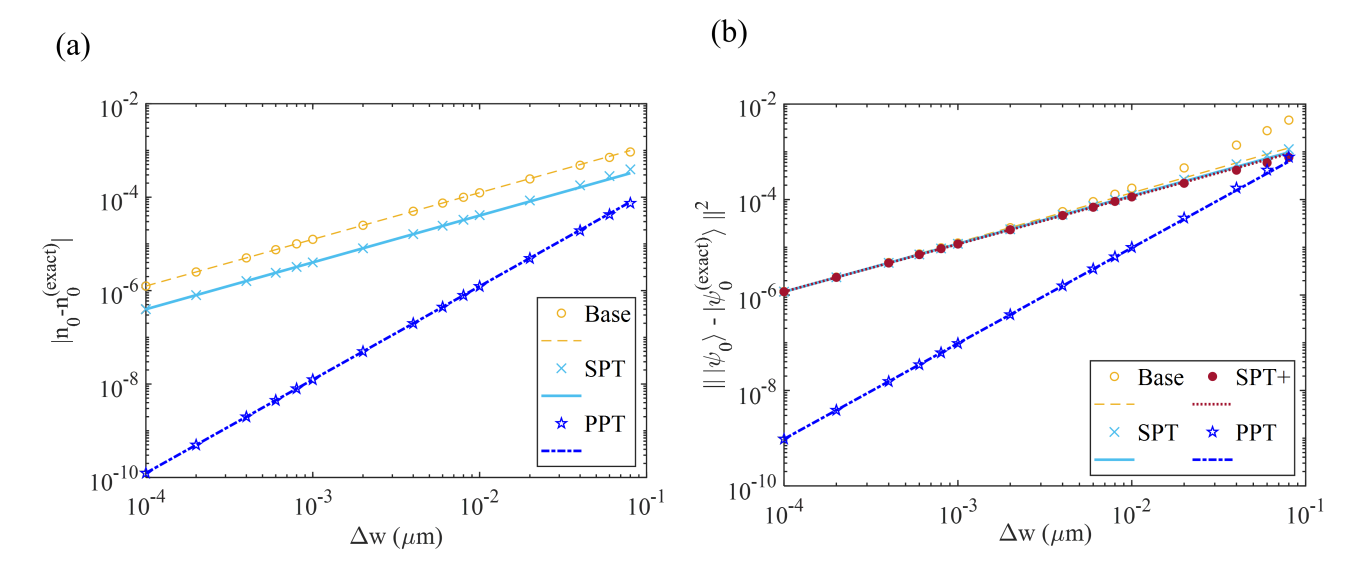


Figure 5: (a) Error in the effective indices of the TM0 mode using the base, SPT and PPT/SPT+ estimations for dilations (Fig. 4(a)), which scale by exponents of 0.999, 1.003, and 1.999 respectively. (b) MSE of the base, SPT, SPT+, and PPT estimations of the mode profiles for dilations which scale by 1.041, 1.007, 0.997, and 2.003 respectively. Recent improvements to standard perturbation theory (SPT), denoted by SPT+, are accurate at estimating effective indices in (a) but not mode profiles in (b).

higher-order TM1 and TM2 modes in respect to a dilation of the waveguide in Fig. 6. While the error increases by  $\sim 3$  dB per mode for both the mode profiles and indices, it is a uniform increase. The mode profiles of SPT+ and mode indices of SPT show a similar uniform 3 dB/mode increase. Additionally, the scale factors are incredibly consistent (standard deviation across the 3 modes is less than 0.001 for all cases) suggesting that even high-order modes can be estimated to arbitrarily high precision.

### Conclusion

We have introduced an improved perturbation theory that accurately captures the case of shifting material interfaces and the concomitant abrupt changes in mode fields and mode indices engendered by the boundary conditions of Maxwell's equations. Such improved perturbation theories become increasingly appealing in today's state-of-the-art photonics where high-index contrast interfaces between nanophotonic structures are commonplace. Bench-

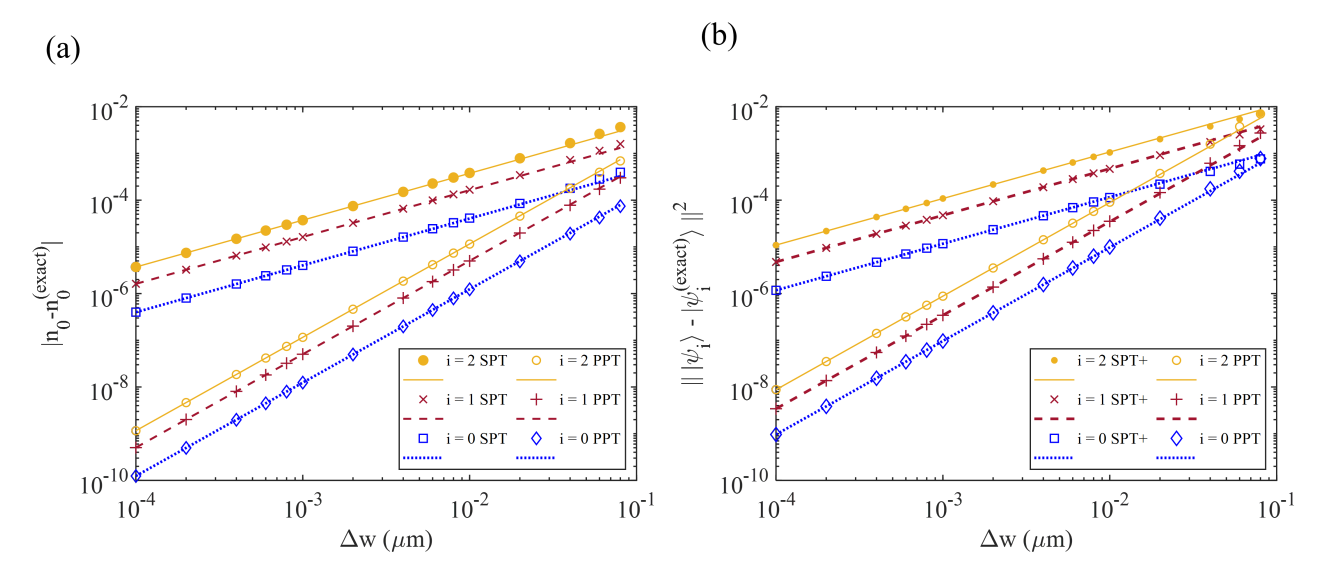


Figure 6: (a) Error in the mode indices of the fundamental, first-order and second-order (i=0, 1, 2) transverse magnetic mode using the SPT and PPT approximations for dilations. SPT errors scale by 1.003, PPT scale by 1.999. SPT+ coincides with PPT for mode indices. (b) MSE corresponding to SPT+ and PPT for dilations of the 0th, 1st, and 2nd TM modes. The SPT+ approximations scale by 0.997, whereas the PPT approximations scale by 2.003.

marking our theory using a multimode silicon waveguide, we showed that our PPT successfully approximates the change in mode profiles and mode indices, unlike the SPT/SPT+ used for typical scalar or low-contrast perturbations which fail at the first order. We anticipate that the demonstrated improvement in calculating mode profiles and mode indices will be of particular benefit in complicated and 3D structures, whereby computationally costly finite-element methods can be avoided for small variations in the cross section or index profiles based on an initially known mode profile. Future work will investigate alternative pacification operations to develop a higher-order PPT, which will assist in the simulation of the propagation of light in devices for which the interfaces change throughout the length of the device, such as in perturbed multimode waveguides <sup>19</sup> alligator photonic crystal waveguides. <sup>22,23</sup> Arbitrary couplings could be implemented amongst the modes, enabling the creation of complex transverse states of light within individual waveguides. This platform can be taken further by using multiple waveguides, such that there can be intrawaveguide modal couplings as well as interwaveguide couplings. Additionally, we expect this formalism can be applied to other

scenarios across physics where the interface between two regions is shifted, like the changes in the effective mass of charge carriers across a heterojunction in condensed matter physics, the finite-quantum well, and other acoustic or mechanical wave phenomena that involve boundaries between dissimilar materials or structures. One can also imagine extending the theory to anisotropic systems where the permittivity tensor is not a scalar, <sup>43,44</sup> or more extensively to non-Hermitian nanophotonics, active lasers, and dissipative systems, where the lack of orthogonality and completeness of eigenstates introduce additional complications. <sup>39,42,45–47</sup>

## Acknowledgement

We thank Rajarshi Roy, Carlos Rìos-Ocampo and Miloš A Popović for valuable discussions. This work was supported by a Faculty-Student Research Award from the University of Maryland, and by a NSF QuSeC-TAQS grant # 2326792.

### References

- (1) Yariv, A. Coupled-mode theory for guided-wave optics. *IEEE Journal of Quantum Electronics* **1973**, *9*, 919–933.
- (2) Gohsrich, J.; Shah, T.; Aiello, A. Perturbation theory of nearly spherical dielectric optical resonators. *Phys. Rev. A* **2021**, *104*, 023516.
- (3) Snyder, A. W.; Love, J. D. Optical Waveguide Theory; Springer US: Boston, MA, 1984.
- (4) Xiong, W.; Hsu, C. W.; Bromberg, Y.; Antonio-Lopez, J. E.; Amezcua Correa, R.; Cao, H. Complete polarization control in multimode fibers with polarization and mode coupling. *Light Sci Appl* 2018, 7, 54.
- (5) Ghatak, A.; Thyagarajan, K. An Introduction to Fiber Optics, 1st ed.; Cambridge University Press: Cambridge, 1998.

- (6) Jalali, B.; Fathpour, S. Silicon Photonics. *Lightwave Technology, Journal of* **2006**, *24*, 4600–4615.
- (7) Guo, X.; Ji, X.; Yao, B.; Tan, T.; Chu, A.; Westreich, O.; Dutt, A.; Wong, C.; Su, Y. Ultra-wideband integrated photonic devices on silicon platform: from visible to mid-IR. *Nanophotonics* **2023**, *12*, 167–196.
- (8) Morse, P. M.; Feshbach, H. *Methods of theoretical physics*; International series in pure and applied physics; McGraw-Hill: New York St Louis San Francisco, 1953.
- (9) Sztranyovszky, Z.; Langbein, W.; Muljarov, E. A. First-order perturbation theory of eigenmodes for systems with interfaces. *Physical Review Research* **2023**, *5*, 013209.
- (10) Weiss, T.; Mesch, M.; Schäferling, M.; Giessen, H. From Dark to Bright: First-Order Perturbation Theory with Analytical Mode Normalization for Plasmonic Nanoantenna Arrays Applied to Refractive Index Sensing. *Physical Review Letters* **2016**, *116*, 237401.
- (11) Lalanne, P.; Coudert, S.; Duchateau, G.; Dilhaire, S.; Vynck, K. Structural Slow Waves: Parallels between Photonic Crystals and Plasmonic Waveguides. ACS Photonics 2019, 6, 4–17.
- (12) Tzuang, L. D.; Soltani, M.; Lee, Y. H. D.; Lipson, M. High RF carrier frequency modulation in silicon resonators by coupling adjacent free-spectral-range modes. *Optics Letters* 2014, 39, 1799–1802.
- (13) Daniel, B. A.; Maywar, D. N.; Agrawal, G. P. Dynamic mode theory of optical resonators undergoing refractive index changes. J. Opt. Soc. Am. B, JOSAB 2011, 28, 2207–2215.
- (14) Dutt, A.; Minkov, M.; Lin, Q.; Yuan, L.; Miller, D. A. B.; Fan, S. Experimental band structure spectroscopy along a synthetic dimension. *Nature Communications* **2019**, *10*, 3122.

- (15) Dong, P.; Preble, S. F.; Robinson, J. T.; Manipatruni, S.; Lipson, M. Inducing Photonic Transitions between Discrete Modes in a Silicon Optical Microcavity. *Physical Review Letters* **2008**, *100*, 033904.
- (16) Dutt, A.; Mohanty, A.; Gaeta, A. L.; Lipson, M. Nonlinear and quantum photonics using integrated optical materials. *Nat Rev Mater* **2024**, *9*, 321–346.
- (17) Almeida, V. R.; Panepucci, R. R.; Lipson, M. Nanotaper for compact mode conversion. Opt. Lett. 2003, 28, 1302–1304.
- (18) Wiederhecker, G. S.; Dainese, P.; Mayer Alegre, T. P. Brillouin optomechanics in nanophotonic structures. *APL Photonics* **2019**, *4*, 071101.
- (19) Mohanty, A.; Zhang, M.; Dutt, A.; Ramelow, S.; Nussenzveig, P.; Lipson, M. Quantum interference between transverse spatial waveguide modes. *Nature Communications* **2017**, *8*, 14010.
- (20) Fried, N.; Dutt, A. Enhanced Control of Intermodal Coupling in Photonic Waveguides. CLEO 2023 (2023), paper JW2A.62. 2023; p JW2A.62.
- (21) Halir, R.; Ortega-Moñux, A.; Schmid, J. H.; Alonso-Ramos, C.; Lapointe, J.; Xu, D.-X.; Wangüemert-Pérez, J. G.; Molina-Fernández, ; Janz, S. Recent Advances in Silicon Waveguide Devices Using Sub-Wavelength Gratings. *IEEE Journal of Selected Topics in Quantum Electronics* 2014, 20, 279–291.
- (22) Hood, J. D.; Goban, A.; Asenjo-Garcia, A.; Lu, M.; Yu, S.-P.; Chang, D. E.; Kimble, H. J. Atom—atom interactions around the band edge of a photonic crystal waveguide. *Proceedings of the National Academy of Sciences* **2016**, *113*, 10507–10512.
- (23) Goban, A.; Hung, C.-L.; Hood, J.; Yu, S.-P.; Muniz, J.; Painter, O.; Kimble, H. Superradiance for Atoms Trapped along a Photonic Crystal Waveguide. *Phys. Rev. Lett.* **2015**, *115*, 063601.

- (24) Moille, G.; Lu, X.; Stone, J.; Westly, D.; Srinivasan, K. Fourier synthesis dispersion engineering of photonic crystal microrings for broadband frequency combs. *Communications Physics* **2023**, *6*, 144.
- (25) Lu, X.; Rao, A.; Moille, G.; Westly, D. A.; Srinivasan, K. Universal frequency engineering tool for microcavity nonlinear optics: multiple selective mode splitting of whispering-gallery resonances. *Photonics Research* **2020**, *8*, 1676.
- (26) Yu, S.-P.; Cole, D. C.; Jung, H.; Moille, G. T.; Srinivasan, K.; Papp, S. B. Spontaneous pulse formation in edgeless photonic crystal resonators. *Nat. Photonics* **2021**, *15*, 461–467.
- (27) Johnson, S. G.; Ibanescu, M.; Skorobogatiy, M. A.; Weisberg, O.; Joannopoulos, J. D.; Fink, Y. Perturbation theory for Maxwell's equations with shifting material boundaries. *Physical Review E* **2002**, *65*, 066611.
- (28) Primo, A. G.; Carvalho, N. C.; Kersul, C. M.; Frateschi, N. C.; Wiederhecker, G. S.; Alegre, T. P. Quasinormal-Mode Perturbation Theory for Dissipative and Dispersive Optomechanics. American Physical Society 2020, 125, 233601.
- (29) Granchi, N.; Intonti, F.; Florescu, M.; García, P. D.; Gurioli, M.; Arregui, G. Q-Factor Optimization of Modes in Ordered and Disordered Photonic Systems Using Non-Hermitian Perturbation Theory. ACS Photoics 2023, 10, 2808–2815.
- (30) Lu, X.; Rogers, S.; Jiang, W. C.; Lin, Q. Selective engineering of cavity resonance for frequency matching in optical parametric processes. Applied Physics Letters 2014, 105, 151104.
- (31) Yan, W.; Lalanne, P.; Qiu, M. Shape Deformation of Nanoresonator: A Quasinormal-Mode Perturbation Theory. *Physical Review Letters* **2020**, *125*, 013901.

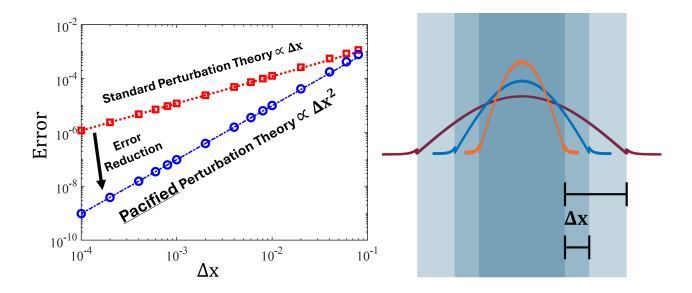
- (32) Skorobogatiy, M.; Ibanescu, M.; Johnson, S. G.; Weisberg, O.; Engeness, T. D.; Soljačić, M.; Jacobs, S. A.; Fink, Y. Analysis of general geometric scaling perturbations in a transmitting waveguide: fundamental connection between polarization-mode dispersion and group-velocity dispersion. *JOSA B* **2002**, *19*, 2867–2875.
- (33) Skorobogatiy, M.; Johnson, S. G.; Jacobs, S. A.; Fink, Y. Dielectric profile variations in high-index-contrast waveguides, coupled mode theory, and perturbation expansions. *Physical Review E* **2003**, *67*, 046613.
- (34) Guerra, G.; Mousavi, S. M. A.; Taranta, A.; Fokoua, E. N.; Santagiustina, M.; Galtarossa, A.; Poletti, F.; Palmieri, L. Unified Coupled-Mode Theory for Geometric and Material Perturbations in Optical Waveguides. *Journal of Lightwave Technology* 2022, 40, 4714–4727.
- (35) McCall, M. et al. Roadmap on transformation optics. *Journal of Optics* **2018**, *20*, 063001.
- (36) Ghojogh, B.; Karray, F.; Crowley, M. Eigenvalue and Generalized Eigenvalue Problems: Tutorial. arXiv, (stat.ML), 2023; https://arxiv.org/abs/1903.11240, (accessed 2024-09-09).
- (37) Svendsen, G. K.; Haakestad, M. W.; Skaar, J. Reciprocity and the scattering matrix of waveguide modes. *Phys. Rev. A* **2013**, *87*, 013838.
- (38) Huang, W.-P.; Mu, J. Complex coupled-mode theory for optical waveguides. *Optics Express* **2009**, *17*, 19134.
- (39) Sternheim, M. M.; Walker, J. F. Non-Hermitian Hamiltonians, Decaying States, and Perturbation Theory. *Phys. Rev. C* **1972**, *6*, 114–121.
- (40) Frankel, T. The geometry of physics: an introduction, 3rd ed.; Cambridge University Press: Cambridge; New York, 2012.

- (41) Huang, X.-Y.; Wang, T.; Liu, S.; Hu, H.-Y.; You, Y.-Z. Quantum Magnetism in Wannier-Obstructed Mott Insulators. *Crystals* **2024**, *14*, 176.
- (42) Sauvan, C.; Wu, T.; Zarouf, R.; Muljarov, E. A.; Lalanne, P. Normalization, orthogonality, and completeness of quasinormal modes of open systems: the case of electromagnetism [Invited]. *Optics Express* **2022**, *30*, 6846.
- (43) Kenig, C. E.; Salo, M.; Uhlmann, G. Inverse problems for the anisotropic Maxwell equations. *Duke Mathematical Journal* **2011**, *157*, 369–419.
- (44) Kottke, C.; Farjadpour, A.; Johnson, S. G. Perturbation theory for anisotropic dielectric interfaces, and application to subpixel smoothing of discretized numerical methods. *Phys. Rev. E* 2008, 77, 036611.
- (45) Shah, T.; Chattopadhyay, R.; Vaidya, K.; Chakraborty, S. Conservative perturbation theory for nonconservative systems. *Phys. Rev. E* **2015**, *92*, 062927.
- (46) Lyu, M.; Gmachl, C. Correction to the effective refractive index and the confinement factor in waveguide modeling for quantum cascade lasers. *OSA Continuum* **2021**, *4*, 2275.
- (47) Gong, Z.; Bello, M.; Malz, D.; Kunst, F. K. Bound states and photon emission in non-Hermitian nanophotonics. *Phys. Rev. A* **2022**, *106*, 053517.

# For Table of Contents Use Only

Title: "Revised perturbation theory for shifting geometric interfaces in high-contrast nanophotonics"

Authors: Nathaniel Fried and Avik Dutt



Right: fundamental modes of an optical waveguide are depicted, which spread out as the waveguide is dilated. Left: reduction in mode calculation error between our pacified perturbation theory compared to standard perturbation theory.